Mass Transfer with Chemical Reaction in Thin-Layer Electrochemical Reactors

Régine Devaux, Alain Bergel, and Maurice Comtat
Laboratoire de Génie Chimique, URA CNRS 192, Université Paul Sabatier, 31062 Toulouse cedex, France

Thin-layer electrochemical reactors are analytical reactors where mass transfers are generally assumed not to affect the overall reaction rate. The validity of this hypothesis was tested for systems involving a second-order or an enzymatic homogeneous reaction that consumed the product generated by the electrochemical heterogeneous reaction. The experiments were performed with the oxidation of hexacyanoferrate II into hexacyanoferrate III, coupled with the consumption of hexacyanoferrate III by the reduced form of nicotinamide adenine dinucleotide, catalyzed or not by a diaphorase. The tools commonly used for gas–liquid interfaces were adapted to the description of mass transfer in a closed thin film. The theoretical model agreed well with the experimental data and served as the basis for testing the thin-layer hypothesis. The validity of the hypothesis was plotted as a function of the Hatta and Damköhler numbers. The influence of concentration and diffusion parameters are discussed with focus on the validity criterion.

Introduction

Description of mass transfers with chemical reaction is a widely investigated topic in the field of gas–liquid interfaces. Astarita (1967) and Danckwerts (1970) proposed complete studies in this area at a very early date. Other authors have broadened the scope of the investigations (Cornelisse et al., 1980; Trambouze, 1981; Charpentier, 1981). Electrochemical engineering can benefit to a large extent from these works because most of the methods and results can be applied directly to the description of mass transfers with chemical reaction at electrochemical interfaces. A great similarity exists between the two kinds of interfaces: in both cases, the essential phenomena occur in the liquid layer adjacent to the interface, where the concentrations are monitored by equilibrium conditions. In gas–liquid systems the interface concentrations are determined by the solubility of the gaseous species; for electrochemical interfaces they are generally determined by the Nernstian equilibrium. As a consequence, the concepts of surface renewal (Tzedakis et al., 1989), Hatta number (Weise et al., 1986), or van Krevelen's representation (Labrune and Bergel, 1992) are, for instance, commonly encountered in electrochemical engineering works.

Nevertheless the case of thin-layer electrochemical reactors seems to have no similarity in the field of gas–liquid interfaces. They are analytical reactors with a very small volume of liquid and a large electrode surface area, resulting in a thickness of approximately the same order of magnitude as a diffusive layer. In the theoretical representation the boundary conditions of the mass balance equations at the side opposite to the electrode indicate that the mass fluxes of all the species are nil at the wall of the reactor. There is no similar case for gas–liquid interfaces because mass transfers are always occurring between the interface layer and the bulk of the solution. The boundary conditions are then determined by the concentrations in the solution. However, gas absorption into a liquid film could be the nearest system to the thin-layer electrochemical setup, but it is generally treated assuming that the penetration thickness is very small with respect to the film thickness (Grossman, 1986; Yih, 1986). In order to perform more efficient absorptions, the film is generally moving, and consequently the concentration gradients do not reach the deep layers far from the interface. The boundary conditions are still determined by the bulk conditions, and they are not affected by the wall that bounds the system, as is the case of thin-layer electrochemical reactors.

Numerous different configurations have been proposed to design thin-layer electrochemical reactors. Devices as simple as porous electrodes, such as graphite felts (Golub and Oren,

Correspondence concerning this article should be addressed to R. Devaux.

1990) or a cylindrical hole in a carbon electrode (Porter and Kuwana, 1984), revealed correct thin-layer behavior. Many reactor setups have also allowed spectrophotometrical measures to be associated with the electrical information. The light beam passes through the transparent electrode and continuously follows the evolution of the spectrum of the solution during the experiment. Many recent works deal with the design of this kind of optically transparent cell (Salbeck, 1992; Brett, 1992). In the current devices the length of the optical path is equal to the thickness of the reactor and, because this thickness is slight, the accuracy of the spectrophotometrical measurements will be affected. This is why numerous attempts are being made in order to increase the length of the optical path without increasing the volume of the reactor (Gui et al., 1991; Wei et al., 1992, 1993). Devices have also been built to allow experiments in organic solvents (Salbeck, 1993) or IR measurement (Yao et al., 1989) to be performed. The method can also be applied, for instance, to the design of efficient detectors for liquid chromatography (Nagy and Anderson, 1991).

Numerous advantages make thin-layer reactors very efficient analytical tools. The volume of solution required is very small and the high value of the electrode surface/reactional volume ratio ensures a rapid change in the concentrations. The formation rate of the electroactive species or, when equilibrium is reached, the ratio of its oxidized and reduced forms can be finely controlled by the appropriate choice of electrode potential. The electrical information is very easy to record and can be straightforwardly correlated to the rate of the reactive process. However, the main advantage of the thin-layer electrochemical reactors is that the mass balance equations are commonly simplified assuming that there is no diffusive limitation (Hubbard and Anson, 1970; Laviron, 1979). The thickness of the reactor is assumed to be small enough to prevent any concentration gradient occurring inside it. All the concentrations are uniform and equal to the concentration at the electrode surface. By means of this "thin-layer" hypothesis, the equations become very easy to solve. Despite the occurrence of an electrochemical step, they are similar to the equations for a homogeneous process in a well-stirred reactor. Coupling spectral and electrical data gives a set of kinetic information that is very easy to process, and particularly fruitful for studying homogeneous reactions preceding or following the electrochemical step, which is controlled by the electrode.

The aim of this article is to propose theoretical and experimental approaches to mass transfer with chemical reaction in a thin quiescent film bounded by an inert wall. The general model was used to check the validity of the thin-layer hypothesis and to improve the exploitation of experimental data obtained with a thin-layer electrochemical reactor. The model was validated with experiments involving the electrochemical oxidation of hexacyanoferrate II into hexacyanoferrate III. The hexacyanoferrate III formed was reduced in solution by nicotinamide adenine dinucleotide (NADH) following second-order homogeneous kinetics. The reaction was further catalyzed by the enzyme diaphorase, resulting in higher reaction rates and more complex kinetics. Such an association between an electrochemical and an enzymatic reaction is often used in biosensors with amperometric detection (Turner et al., 1987).

Theory

Physical description

Most of the reactors have flat electrodes. A classic and widely used setup consists of two metallic electrodes spaced by a micrometer (Hubbard and Anson, 1970), but this does not allow a spectrophotometric measurement to be easily recorded. Here we preferred to use a transparent electrode consisting of a platinum grid inserted between two parallel glass slides bonded together (Heineman et al. 1975). The volume of the solution retained between the two glass slides was a few tens of microliters, for a geometric surface area of the electrode of about 1 cm^2. The light beam passed through the glass slides perpendicularly to the grid electrode. The potential of the electrode was maintained at a constant value with respect to a reference electrode. The spectra of the solution were recorded continuously during electrolysis, allowing the evolution of the concentration of each species to be plotted as a function of time. In all the experiments the electrochemical reaction consisted of the oxidation of an electrochemical mediator (Red) at the surface electrode:

$$\text{Red} <\!\!-\!\!-\!\!> Ox + ne.$$

The homogeneous reaction was the consumption by a reagent (S) of the oxidized form of the mediator, which was electrochemically generated. The notation S was used for the reagent because it is called substrate when it is involved in a biochemical reaction:

$$\gamma S + Ox \rightarrow \gamma P + \text{Red}.$$

The reaction was either of the second order

$$r = k[S][Ox], \tag{1}$$

or catalyzed by an enzyme, with Michaelis–Menten kinetics

$$r = \frac{k_e[E]}{1 + \dfrac{K_S}{[S]} + \dfrac{K_{Ox}}{[Ox]}}, \tag{2}$$

where $k_e[E]$ represents the activity of the enzyme. This is the maximum rate that would be obtained with high concentrations of S and Ox compared to the Michaelis constants K_S and K_{Ox}, respectively. This activity can be expressed in $M \cdot s^{-1}$, or in the usual biochemical unit (U/mg) for the specific activity, which corresponds to the micromoles of NADH consumed per minute and per milligram of enzyme.

Mass balance equations

The simplest representation of a flat, thin-layer electrochemical reactor is a film bounded by the electrode on one side and an inert wall on the other side (Figure 1). Using dimensionless variables, the general transient mass balance equations for a second-order reaction were

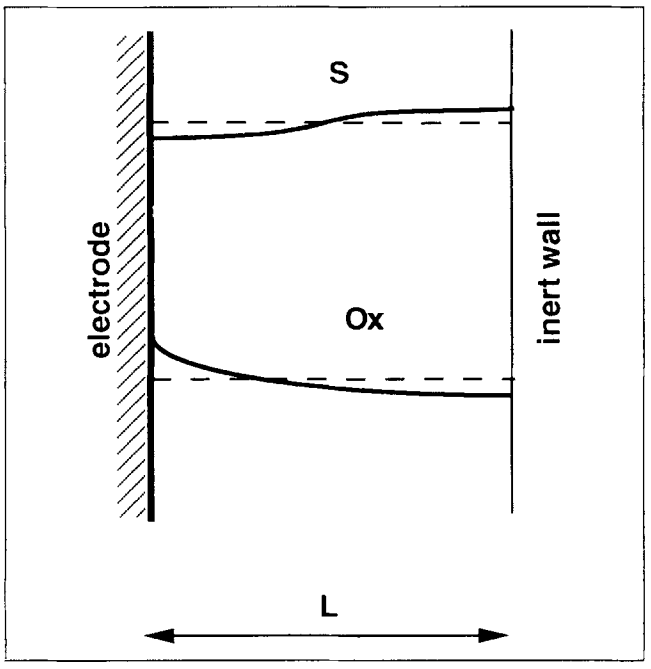

Figure 1. Thin-layer electrochemical reactor.

Concentration profiles of the substrate and the mediator are plotted as a function of the distance from the electrode: dotted and full dashed lines represent, respectively, the thin-layer model and the diffusive one.

$$\frac{\partial S}{\partial T} = D\frac{\partial^2 S}{\partial X^2} - \gamma Ha^2 Ox S \tag{3}$$

$$\frac{\partial Ox}{\partial T} = \frac{\partial^2 Ox}{\partial X^2} - Ha^2 Ox S, \tag{4}$$

where

$$D = \frac{D_S}{D_{Ox}} \tag{5}$$

$$Ha^2 = \frac{k[S]^0 L^2}{D_{Ox}}. \tag{6}$$

The Hatta number expresses the ratio of the potential homogeneous reaction rate without any mass transport limitation, to the maximal diffusion rate of the mediator. The same form was kept for the enzymatic kinetics:

$$\frac{\partial S}{\partial T} = D\frac{\partial^2 S}{\partial X^2} - \gamma Ha'^2 \frac{\mathrm{Red}^0}{1 + \frac{K'_S}{S} + \frac{K'_{Ox}}{Ox}} \tag{7}$$

$$\frac{\partial Ox}{\partial T} = \frac{\partial^2 Ox}{\partial X^2} - Ha'^2 \frac{\mathrm{Red}^0}{1 + \frac{K'_S}{S} + \frac{K'_{Ox}}{Ox}}, \tag{8}$$

where

$$Ha'^2 = \frac{k_e[E]L^2}{D_{Ox}[\mathrm{Red}]^0} \qquad K'_S = \frac{K_S}{[S]^0} \qquad K'_{Ox} = \frac{K_{Ox}}{[S]^0}. \tag{9-11}$$

The strict definition of Ha would lead to

$$Ha^2 = \frac{k_e[E]L^2}{D_{Ox}[\mathrm{Red}]^0} \cdot \frac{1}{1 + \frac{K'_S}{S} + \frac{K'_{Ox}}{Ox}},$$

but we preferred to use the maximal value Ha' for the sake of simplicity.

Initially only the substrate and the reduced form of the mediator were present in solution:

$$S^0 = 1 \qquad \mathrm{Red}^0 = \frac{[\mathrm{Red}]^0}{[S]^0} \qquad Ox^0 = 0. \tag{12-14}$$

According to this initial condition and assuming that the diffusivities of the reduced and oxidized forms of the mediator are equal led to:

$$Ox + \mathrm{Red} = \mathrm{Red}^0 \tag{15}$$

At the inert wall ($X = 1$) all the mass fluxes were nil:

$$\frac{\partial S}{\partial X}\Big|_{X=1} = 0 \qquad \frac{\partial Ox}{\partial X}\Big|_{X=1} = 0. \tag{16-17}$$

The boundary conditions at the electrode surface ($X = 0$) are determined by the electrochemical conditions. At the chosen potential the substrate was not electroactive:

$$\frac{\partial S}{\partial X}\Big|_{X=0} = 0 \tag{18}$$

The mass flux of the mediator was controlled by the oxidation rate

$$-D_{Ox}\frac{\partial [Ox]}{\partial x}\Big|_{x=0} = k_f[\mathrm{Red}]|_{x=0} - k_b[Ox]|_{x=0}, \tag{19}$$

where k_f and k_b are the forward and backward constants relative to the electrochemical oxidation of the mediator. These variables are monitored by the potential according to:

$$k_f = k_0 \exp\left[\frac{(1-\alpha)nF}{RT}(E - E'_0)\right] \tag{20}$$

$$k_b = k_0 \exp\left[\frac{-\alpha nF}{RT}(E - E'_0)\right], \tag{21}$$

where k_0 is the rate constant of the heterogeneous electronic transfer, α the transfer coefficient, and E'_0 the normal apparent potential. With dimensionless variables, the boundary condition became

$$\frac{\partial Ox}{\partial X}\Big|_{X=0} = Da\xi^{-1}[Ox|_{X=0}(1+\xi) - \xi \mathrm{Red}^0], \quad (22)$$

where

$$\xi = \exp\left[\frac{nF}{RT}(E - E'_0)\right] \quad (23)$$

$$Da = \frac{k_f L}{D_{Ox}}. \quad (24)$$

The Damköhler number expresses the ratio of the potential heterogeneous reaction rate without any mass transport limitation, to the maximal diffusion rate of the mediator.

It should be noted that one of the advantages of electrochemistry is that it offers the possibility of finely controlling the value of the Damköhler number, since

$$Da = \frac{k_0 \xi^{1-\alpha} L}{D_{Ox}}. \quad (25)$$

In most of the studies the electrochemical reaction is assumed to be very fast compared to the mass transfers and the homogeneous reactions. This assumption leads to the Nerstian equilibrium at the surface of the electrode, expressed by

$$\frac{Ox|_{X=0}}{\mathrm{Red}|_{X=0}} = \frac{k_f}{k_b} = \xi. \quad (26)$$

The equations were solved numerically by a classic finite difference method. The concentration profiles were integrated inside the cell by a Simpson's method to calculate the average concentration value, which was obtained experimentally by the spectrophotometric measure:

$$\bar{S} = \int_0^1 S dX \quad \overline{Ox} = \int_0^1 Ox dX. \quad (27\text{-}28)$$

When the "thin-layer" hypothesis is used, it is assumed that no diffusive step affects the reaction rate, and that, consequently, no concentration gradient occurs in the reactor. The regeneration of the mediator, Ox, performed by the electrochemical oxidation at the electrode, is then very fast compared to the other steps, and results in a constant and uniform concentration of Ox being kept during electrolysis. The mass balance equations for a second-order reaction became:

$$\overline{Ox} = Ox|_{X=0} \quad (29)$$

$$\frac{\partial \bar{S}}{\partial T} = -\gamma Ha^2 \overline{Ox}\bar{S}, \quad (30)$$

which led to

$$\overline{Ox} = \mathrm{Red}^0 \frac{\xi}{1+\xi} \quad (31)$$

$$\bar{S}(T) = \exp(-\gamma Ha^2 \overline{Ox} T). \quad (32)$$

In the same way, the following was obtained for the enzymatic catalysis:

$$\overline{Ox} = \mathrm{Red}^0 \frac{\xi}{1+\xi} \quad (33)$$

$$-\gamma Ha'^2 \mathrm{Red}^0 T = \left(1 + \frac{K'_{Ox}}{\overline{Ox}}\right)(\bar{S} - 1) + K'_S \ln \bar{S}. \quad (34)$$

When ohmic drop had to be taken into account, the expression of the rate constants (Eqs. 20 and 21) were modified:

$$k_f = k_0 \exp\left[\frac{(1-\alpha)nF}{RT}(E - E'_0 - R_\Omega I)\right] \quad (35)$$

$$k_f = k_0 \exp\left[\frac{-\alpha nF}{RT}(E - E'_0 - R_\Omega I)\right], \quad (36)$$

where R_Ω is the uncompensated cell resistance and I the current intensity given by Fick's law:

$$I = -nFAD_{ox}\frac{\partial [Ox]}{\partial x}\Big|_{x=0}, \quad (37)$$

where A is the electrode surface area.

Experiment

Hexacyanoferrate II and III, nicotinamide adenine dinucleotide, and diaphorase from *Clostridium kluyveri* (E.C. 1.8.1.4) were purchased from Sigma. All the experiments were carried out in a phosphate buffer 0.2 M, pH 7.5.

The thin-layer reactor consisted of two parallel glass slides bonded together with the working electrode inserted between them. The working electrode was a platinum grid purchased from Comptoir Lyon Alemand Louyot, 1,024 meshes/cm^2 woven with a 0.06-mm-dia. wire. The ends of the slides were dipped into a 400-μL beaker in which another platinum grid used as auxiliary electrode was immersed. The saturated calomel reference electrode (SCE) was connected with the solution in the beaker by a capillary filled with the buffer solution (Luggin capillary). The potential of the working electrode was monitored with respect to the reference electrode by means of a potentiostat (Tacussel, PRT 20×2X). The thin-layer cell was placed in the compartment of a spectrophotometer. The Hewlet-Packard (type 8451) diode array spectrophotometer allowed a spectrum to be recorded and stored in only a few seconds. Spectra of the solution were thus recorded at regular time intervals varying from 10 to 60 s, according to the total electrolysis time.

The solution resistivity (ρ) was measured with a conductimeter (Tacussel, CDRV G2) and a probe (Tacussel, XE 153/230). The resistance (R_Ω) was calculated by means of the equation:

$$R_\Omega = \frac{\rho d}{S}, \quad (38)$$

where S is the cross section of the thin layer cell ($S = 0.15$ cm^2) and d the distance between the working electrode and the top of the Lugin capillary ($d = 0.5$ cm).

The activity of the diaphorase was measured independently of the electrochemical experiments. The oxidation of NADH by hexacyanoferrate III was performed in a 600-μL spectrophotometric cell, with the initial concentrations: 2-mM NADH; 2-mM $Fe(CN)_6^{3-}$. Evolution of the concentration of hexacyanoferrate III was followed at 420 nm. Only a slow decrease of the concentration was measured. When the rate of hexacyanoferrate III consumption had stabilized at a constant value, 10 μL of solution of diaphorase (0.5 mg/mL) were introduced into the cell. The difference between the slopes of the absorbance curves as a function of time before and after the addition of enzyme gave the specific activity of the diaphorase ($A_E = 25$ U/mg), which led to

$$k_e[E] = A_E \cdot C_E, \tag{39}$$

where C_E is the enzyme weight concentration.

The exact volume (V) and thickness (L) of the reactor were determined by separate experiments carried out with only 30-mM hexacyanoferrate III in solution. The potential was no longer maintained at a constant value during electrolysis, but was varied with a slow constant scan rate ($s = 1$ mV/s) by means of a signal generator (Tacussel, servovit). The current was recorded as a function of the potential. The curve exhibited a peak whose intensity (I_p) is given by the expression (Bard and Faulkner, 1980):

$$I_p = \frac{n^2F^2 \mid s \mid V[Fe(CN)_6^{3-}]}{4RT}. \tag{40}$$

The experimental value of the peak intensity gave the volume of the reactor. During this experiment hexacyanoferrate underwent successive complete oxidations and reductions. The absorbance difference at 420 nm (ΔA^{420}) between the two states was:

$$\Delta A^{420} = \epsilon \cdot L \cdot C \tag{41}$$

with $\epsilon = 1.04$ mM$^{-1}\cdot$cm^{-1} and $C = 30$ mM. This equation gave the thickness of the cell.

Results and Discussion

The electrochemical mediator (Red/Ox), hexacyanoferrate II/hexacyanoferrate III, underwent oxidation at the electrode:

$$Fe(CN)_6^{4-} <\!\!-\!\!-\!\!> Fe(CN)_6^{3-} + e.$$

The hexacyanoferrate III generated is then consumed by the coupled homogeneous reaction involving the reduced form of nicotinamide adenine dinucleotide (NADH):

$$\frac{1}{2}NADH + Fe(CN)_6^{3-} \longrightarrow \frac{1}{2}NAD^+ + Fe(CN)_6^{4-} + \frac{1}{2}H^+.$$

Table 1. Extinction Coefficient of NADH and Hexacyanoferrate III

Wavelength (nm)	Extinction Coefficient (mM$^{-1}\cdot$cm^{-1})	
	ϵ_{NADH}	$\epsilon_{hexacyanoferrate\ III}$
340	6.22	0.55
420	0.00	1.02

Only hexacyanoferrate II ($Fe(CN)_6^{4-}$) and NADH were initially present in the solution to prevent any reaction from occurring before the potential of the electrode was set to +0.30 V with respect to the reference electrode. The concentrations of hexacyanoferrate III and NADH were determined by means of the absorbance measurements at 420 nm and 340 nm. They correspond to the maximum absorption of hexacyanoferrate III and NADH, respectively, with the extinction coefficients reported in Table 1. The absorbance, at each wavelength, was the resultant of three components due to:

- The residual absorbance of the cell: A_{resid}, which is generally not negligible because the light beam passed through the grid electrode
- Hexacyanoferrate III: A_{Ox}
- NADH: A_S.

Hexacyanoferrate II and the oxidized form NAD^+ did not absorb in this range. The general expressions of the absorbances at time t were then

$$A_t^{340} = A_{resid}^{340} + A_{Ox}^{340} + A_S^{340} \tag{42}$$

$$A_t^{420} = A_{resid}^{420} + A_{Ox}^{420}. \tag{43}$$

Given that $A_{Ox} = 0$ at the beginning of the reaction ($t = 0$), because only hexacyanoferrate II was in solution, and that $A_S = 0$ at the end ($t = \infty$), because the reaction was pursued until all the NADH was consumed, the concentrations of hexacyanoferrate III (Ox) and NADH (S) were given by

$$[Ox] = \frac{A_{Ox}^{420}}{L\epsilon_{Ox}^{420}} \qquad [S] = \frac{A_s^{340}}{L\epsilon_S^{340}} \tag{44-45}$$

with

$$A_{Ox}^{420} = A_t^{420} - A_{t=0}^{420} \tag{46}$$

$$A_S^{340} = A_t^{340} - A_{Ox}^{420} \cdot \frac{\epsilon_{Ox}^{340}}{\epsilon_{Ox}^{420}} - A_{resid}^{340} \tag{47}$$

$$A_{resid}^{340} = A_{t=\infty}^{340} - A_{Ox\,t=\infty}^{340} \tag{48}$$

Second-order homogeneous reaction

Figure 2 represents the concentration evolutions of $\overline{S}$ and $\overline{Ox}$ as a function of time for different values of the concentration parameter $Red^0 = [Red]^0/[S]^0$. According to the thin-layer hypothesis, the concentration of the oxidized mediator $\overline{Ox}$ would be constant with respect to time, and equal to the equilibrium concentration monitored by the potential of the electrode $Red^0(\xi/(1+\xi))$. The experimental curves showed

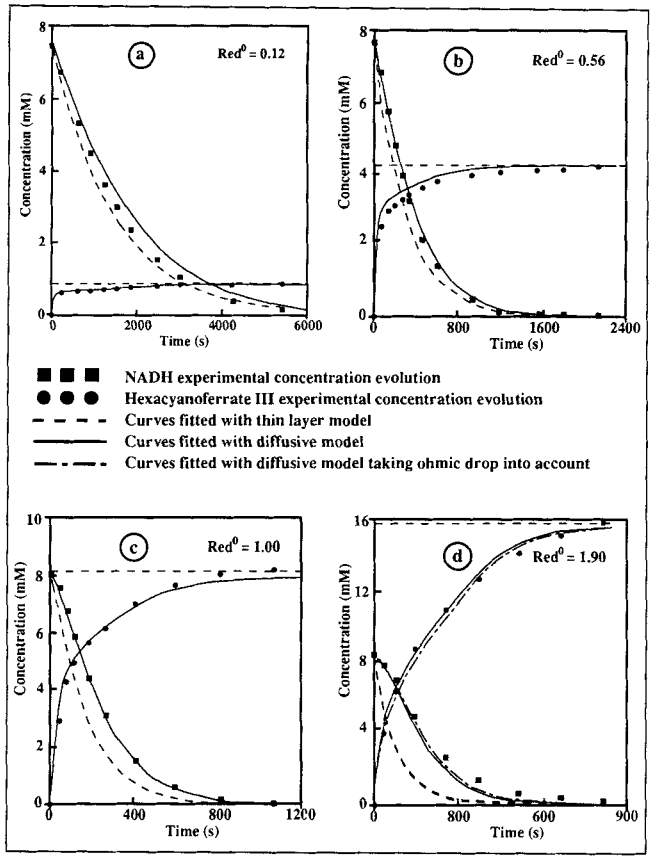

Figure 2. Concentration evolutions of substrate and mediator.

NADH and hexacyanoferrate III experimental concentrations are plotted as a function of time and are fitted with the thin-layer and diffusive models (without or with taking ohmic drop into account). Experimental and adjusted parameters are gathered in Table 2.

that this hypothesis was not verified at the onset of the reaction. An initiation period was necessary for the electrochemical reaction to ensure a uniform equilibrium concentration in the reactor. Without any homogeneous reaction coupled to the electrochemical step, this corresponds to the establishment of a diffusive layer from the electrode to the wall of the cell. It is known that the diffusive layer is well-established after a time t_d ($t_d >> L^2/2D_{ox}$) (Bard and Faulkner, 1980). Comparison of the experimental curves shows that, during this time, the higher the Red^0 value was, the more rapidly the substrate was consumed. This explains why the thin-layer model correctly fitted the experimental data for the lowest values of Red^0, while it became less and less valid as Red^0 increased. The kinetic constant k of the homogeneous reaction was adjusted to 1.55 $M^{-1}\cdot s^{-1}$ using only the curves obtained with low Red^0 values. On the other hand, the diffusive model based on the general mass balance equations appeared quite correct, since it succeeded in fitting the evolution of the concentration curves whatever the Red^0 value. All the values of the parameters used in the simulation were extracted from the literature (Table 2), except the kinetic constant k, which was kept at the same value as found previously. The heterogeneous constant k_0 was the only parameter to be adjusted by means of the *Da* number. An empirical

Table 2. Experimental and Adjusted Parameters for the Second-Order Homogeneous Reaction

E (mV/ECS)	E'_0	ξ	α	D_{Ox} $(m^2/s)\times10^{10}$	D_S	D	γ
300	195*	60	0.5	11.83†	2.4‡	0.2	0.5

Experimental				Adj.
$[S]^0$ (mM)	Red^0	L(m) $\times10^4$	Ha	Da
7.5	0.12	3.7	1.16	> 1.30
7.7	0.56	3.0	0.95	0.23
8.0	1.00	3.0	0.97	0.05
8.3	1.90	3.0	0.99	0.02

*Durliat (1975).
†Weast et al. (1987).
‡Aizawa et al. (1975).

trial and error procedure was used. For the lowest values of Red^0, only high values of k_0 made it possible to fit the experimental data. The *Da* number must be higher than approximately 1; the electrochemical reaction was in this case very fast compared to the diffusive phenomena, and it did not affect the overall reaction rate. Surprisingly it was necessary to reduce the value of k_0 when Red^0 increased. Actually this phenomenon has already been shown: the heterogeneous transfer rate constant of the couple $Fe(CN)_6^{3-}/Fe(CN)_6^{4-}$ decreases as a function of the concentration (Kawiak et al., 1983). Table 3 shows some similarity between the variation of k_0 as found in our simulation and as reported in the literature. The discrepancy between the variation ranges is certainly due to the very different operating conditions that induced very different states of the electrode surface. Indeed the variation of k_0 is certainly caused by surface modifications rather than by an intrinsic variation of the electron transfer rate. Besides, the influence of the surface features on the apparent rate constant has been extensively studied in the case of biological molecules (Bond and Hill, 1991).

The influence of ohmic drop was estimated for the experiment performed with the greatest mediator concentration ($Red^0 = 1.9$). Equations 35 and 36 were used to calculate the values of k_f and k_b, respectively, with the value of the resistance determined experimentally ($R_\Omega = 160\ \Omega$). The two curves in Figure 2d are fitted with the same parameter values, with or without taking ohmic drop into account. Because of the slight effect for the curve obtained with the highest current, ohmic drop was subsequently neglected.

Table 3. Heterogeneous Transfer Rate Constants for Hexacyanoferrate System

Conc. (mM)	k_0 $(cm\cdot s^{-1})$		Background (Electrolyte)	Data from
15.8	5.8	10^{-5}		
8.0	1.6	10^{-4}	KH_2PO_4	This paper
4.3	7.1	10^{-4}	0.2 M	
0.9	> 3.2	10^{-3}		
2.0	2.9	10^{-2}		
0.5	4.1	10^{-2}	$MgCl_2$	Kawiak (1983)
0.2	6.1	10^{-2}	0.05M	
0.1	8.2	10^{-2}		

In order to check the validity of the thin-layer hypothesis in general, a criterion had to be chosen. The error in the halfway reaction time ($\Delta T_{1/2}$) was a simple parameter, which is particularly sensitive to the onset of the reaction, that is, the greater the time necessary for the *Ox* concentration to reach the equilibrium value, the higher the error $\Delta T_{1/2}$. Figure 3 reports the variation of the halfway reaction time as a function of the Hatta number for the thin layer and the diffusive models for a general case, with $D = 1$ and $\gamma = 1$. When *Ha* was less than one, the thin-layer approximation was valid. As shown on the concentration profiles plotted with $Ha = 0.3$, no significant gradient occurred in the cell. On the other hand, for higher values of *Ha* the rate of substrate consumption no longer increased because the diffusive transfers became rate limiting. Plotting the concentration profiles with $Ha = 10$ clearly showed the effect of diffusion. The rate of the electrochemical step also affects the overall rate when the Damköhler number decreased below approximately 0.1. It was not possible to recover the limit case of "instantaneous" reaction as it is in gas-absorption systems. Because of the high concentration of substrate with respect to the mediator that is generally used, the reaction plane would be located very near the electrode surface. This case would be similar to a surface reaction on the substrate. The validity domain of the thin-layer hypothesis is reported in Figure 4 as a function of *Ha* and *Da*, assuming that the hypothesis remained correct and provided that the discrepancy between the two values of the halfway reaction time was lower than 10%. The frontiers were determined with a numerical dichotomy method: for each value of *Da*, the value of *Ha* was calculated, which led to 10% for $\Delta T_{1/2}$ (Figure 4, curves 1, 2, and 3). The validity of the thin-layer hypothesis cannot be very significantly enlarged if a less severe criterion is used. When a 20% error instead of 10% error was accepted on the halfway reaction time, the stability domains were only slightly shifted to higher values of *Ha*. The higher validity frontier calculated for $Red^0 = 0.1$ and $D = 1$ went from $Ha = 0.62$ to $Ha = 0.95$ (Figure 4 curves 2 and 4). It clearly appeared that the experimental data could be exploited by means of this hypothesis only in the restricted domain of slow homogeneous reactions: a lower value of Red^0 slightly enlarged the domain.

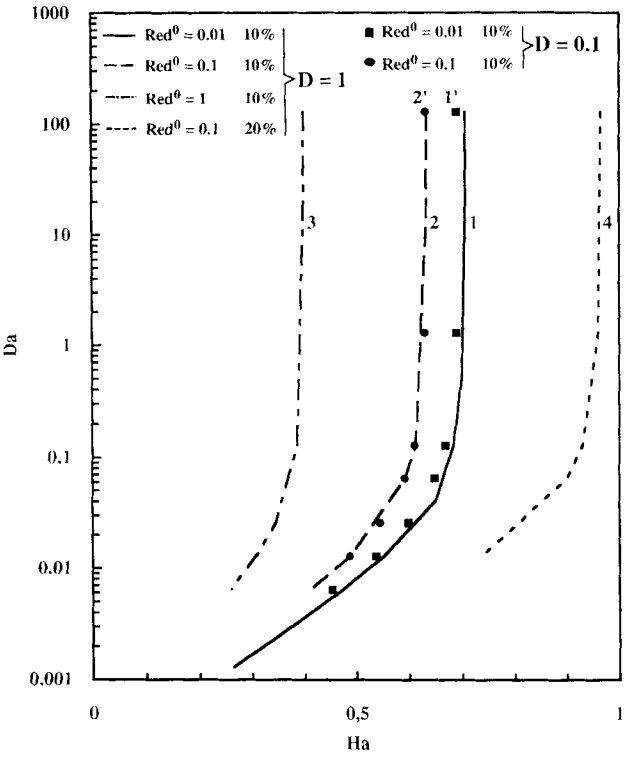

Figure 4. Validity domains of the thin-layer hypothesis with the error $\Delta T_{1/2}$ as criterion.

Theoretical *Da*/*Ha* curves are drawn for different values of Red^0, of *D*, and of the percentage of the error on $T_{1/2}$. $\gamma = 1$.

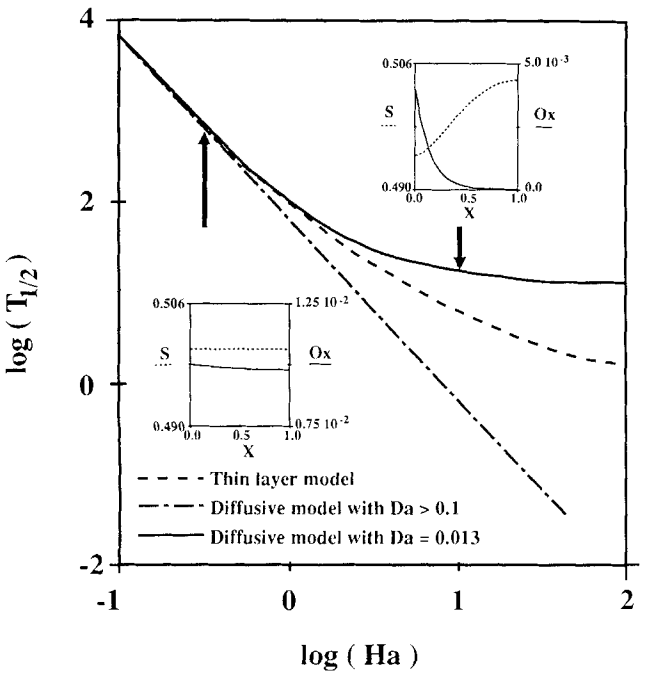

Figure 3. Time of halfway reaction evolutions.

$T_{1/2}$ is plotted as a function of the Ha number for the thin-layer model and the diffusive one with or without the influence of the Damköhler number. *S*/*X* and *Ox*/*X* curves are plotted for two values of *Ha*(*Ha* = 0.3 and *Ha* = 10). $D = 1$, $\gamma = 1$, $Red^0 = 0.01$.

In classic systems where mass fluxes occur between the bulk of the solution and the interface layer, the influence of the concentration parameter Red^0 and of the diffusion parameter, $D = D_S/D_{Ox}$, is quite similar, and is taken into account by means of only one concentration-diffusion parameter (Charpentier, 1981):

$$Zd = \left(\frac{D_S}{\gamma D_{ox}}\right)\left(\frac{[S]}{[Ox]}\right) = \frac{D}{\gamma \mathrm{Red}^0}. \qquad (49)$$

Figure 4 shows that the diffusion parameter *D* had a lesser influence here than the concentration parameter Red^0 (curve 1′ compared to curves 1 and 2, and curve 2′ compared to curves 2 and 3). This behavior seems to be specific to mass transfer in thin closed systems.

The criterion chosen was perhaps not in good agreement with common practice. As is the case in Figure 5, it is usual

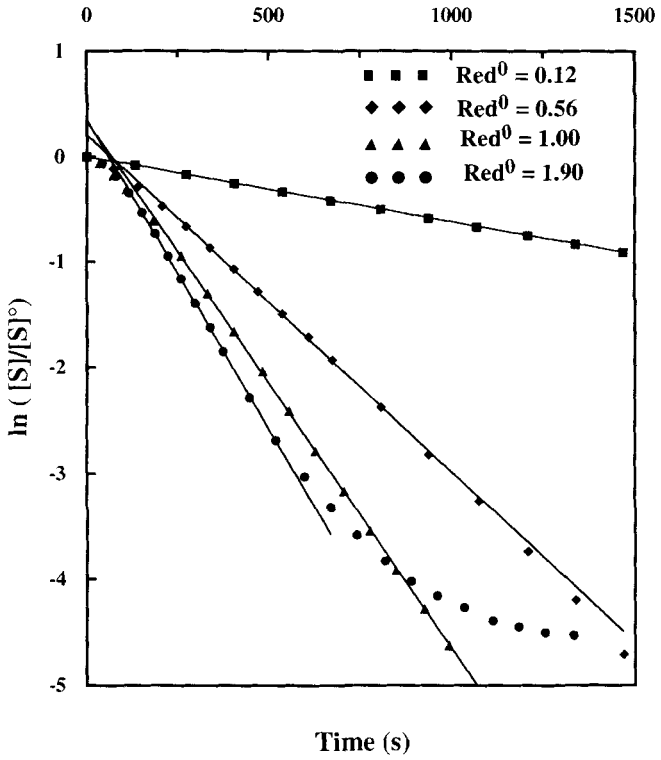

Figure 5. Logarithmic substrate concentration as a function of time.

The logarithmic NADH concentrations are plotted as a function of time. The linear part of the experimental curves are extrapolated (lines). Experimental conditions are gathered in Table 2.

to plot the logarithm of the substrate concentration as a function of time, and to further exploit only the linear part of the curves according to the thin-layer hypothesis:

$$\ln\left(\frac{[S]}{[S]^0}\right) = -\gamma k[Red]^0 \frac{\xi}{(1+\xi)} t. \qquad (50)$$

This method makes it possible not to take into account the onset of the reaction. It is thus normal that the extrapolation of the linear part of the curves does not pass through the zero point of the graph. With this method it was possible to calculate the correct value of the kinetic constant k, even with the experimental data obtained when the thin-layer hypothesis was not strictly valid at the beginning of the reaction. In order to translate this usual operating method into a numerical criterion, it is assumed that the thin-layer hypothesis is valid when 50% of the equilibrium concentration is reached for $\overline{Ox}$, before half of the substrate has been consumed. According to the strict thin-layer hypothesis, the electrochemical step would ensure the equilibrium value from the onset of the reaction and throughout the whole reaction time. Nevertheless, in reality the concentration variation from the initial state to equilibrium takes a certain time. This criterion is not very strict because only 50% of the equilibrium is supposed to be necessary to apply the thin-layer model. The C/t curves, where the minimum of 50% of the equilibrium is reached after the halfway reaction time, are rejected for thin-layer fitting. It seems valid to exploit at least the second part of the curve. The validity domain is thus defined as the domain where the second part of the reaction is performed with at least 50% of the equilibrium concentration for $\overline{Ox}$. The new validity domains are plotted in Figure 6. The domains kept the same overall shapes as previously and the validity of the thin-layer hypothesis remained quite restricted, even with a rather relaxed criterion, which is closer to the usual practice of experimentalists than the previous stricter criterion.

Enzymatic homogeneous reaction

Thin-layer electrochemical reactors are particularly useful tools in the field of analytical biochemistry. According to the thin-layer hypothesis, the Ox concentration would be constant and uniform in the reactor, and the complex enzymatic kinetics could become:

$$r = \frac{k_e[E]}{1 + \frac{K_S}{[S]} + \frac{K_{Ox}(1+\xi)}{[\mathrm{Red}]^0 \xi}}. \qquad (51)$$

In this case, electrochemistry is able to monitor the catalytic activity of the enzyme. Moreover, if the concentration of S is high enough for the ratio $K_S/[S]$ to be negligible with respect to one, the catalytic rate becomes constant: the evolution of the substrate concentration would then be straightfor-

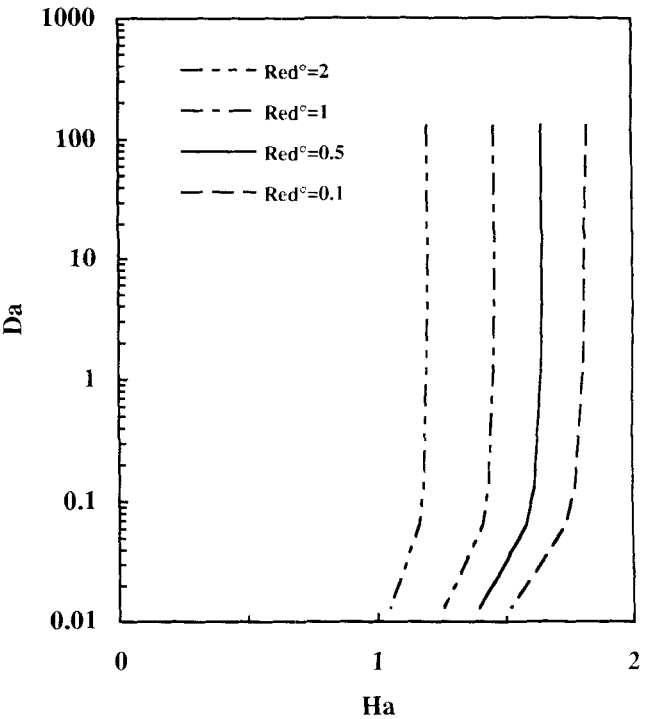

Figure 6. Validity domains of the thin-layer hypothesis with the criterion: 50% of the equilibrium mediator concentration is reached before half of the substrate had been consumed.

Theoretical *Da/Ha* curves are drawn for different values of Red^0. $D = 1$, $\gamma = 1$.

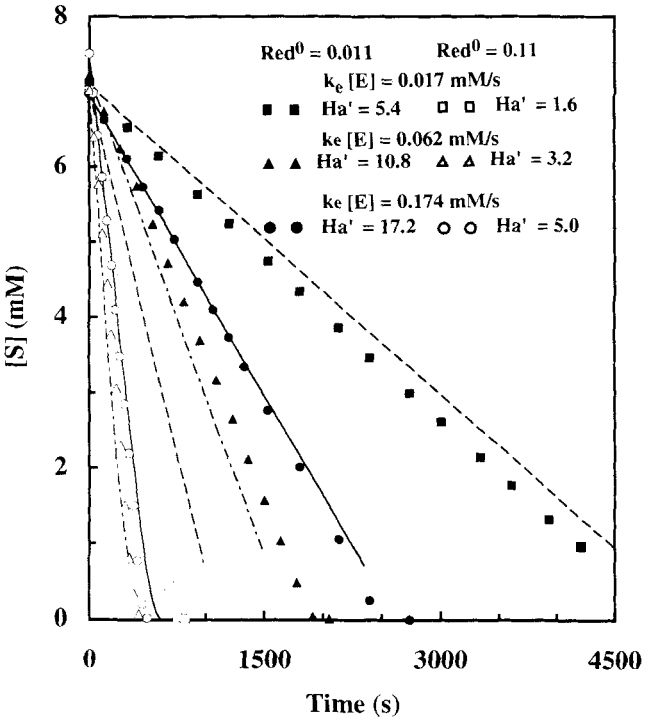

Figure 7. Concentration evolutions of substrate for the enzymatic reaction.

NADH concentrations are plotted as a function of time and are fitted with the diffusive models (lines) for different values of hexacyanoferrate and diaphorase concentrations. $D = 0.2$, $\gamma = 0.5$, $K'_{Ox} = 0.007$, and $K'_S = 0.014$.

ward as a function of time. It has to be mentioned that the capability of electrochemistry to ensure a high concentration of the mediator involved in an enzymatic catalysis has often been used to drive enzymatic synthesis or to shift enzymatic equilibrium (Bauer et al., 1981; Lortie et al., 1992; Chen and Nobe, 1993).

The changes in the substrate concentration as a function of time when different amounts of enzyme were added in the reactor are plotted in Figure 7. The activity of the enzyme, $k_e[E]$, proportional to the amount contained in solution, was experimentally measured. The thin-layer model gives the following equation:

$$\left(1+\frac{K_{Ox}}{[Ox]}\right)([S]-[S]^0)+K_s \ln\left(\frac{[S]}{[S]^0}\right) = -\gamma k_e[E]t, \quad (52)$$

that is, with dimensionless parameters

$$\left(1+\frac{K'_{Ox}}{Ox}\right)(S-1)+K'_S \ln S = -\gamma Ha'^2 \,\mathrm{Red}^0 T, \quad (53)$$

which leads to Eqs. 54–55 when $K_S\,[Ox]$ or K'_S is very small.

$$\left(1+\frac{K_{Ox}}{[Ox]}\right)([S]-[S]^0) = -\gamma k_e[E]t, \quad (54)$$

that is, with dimensionless parameters

$$\left(1+\frac{K'_{Ox}}{Ox}\right)(S-1) = -\gamma Ha'^2 \,\mathrm{Red}^0 T \quad (55)$$

with $[Ox]$ or Ox as a constant value $[Ox]=[\mathrm{Red}]^0\ \xi/(1+\xi)$ or $Ox = \mathrm{Red}^0\ \xi/(1+\xi)$.

Although all the curves were linear up to conversion ratios as high as 90%, as indicated by the thin-layer model (Eqs. 54–55), it cannot be concluded that this hypothesis is valid. Let us define the relative error on the slope of the evolution curves as the ratio $(S_{tl} - S_d)/S_d$, where S_{tl} is the slope predicted by the thin layer theory, and S_d the value calculated by the diffusive model. Actually this ratio is a theoretical estimation between the two models. It is plotted on Figure 8 as a function of Ha with the experimental values of the parameter $D = 0.2$ and $\gamma = 1/2$. The values of Da were those calculated in the first part of the work for the same hexacyanoferrate concentrations. The value of $K_S = 0.1$ mM was found in the literature for various types of diaphorase (Barman, 1985). It was verified that this parameter only affected the shape of the curves slightly because the ratio $K_S/[S]$ could be neglected until very high values of the conversion ratio were reached. The curves indicated that the discrepancy between the thin layer and the diffusive models was very important for the values of Ha used in the experiments. Indeed each curve in Figure 7 was fitted separately by the thin-layer model. For each curve the value of the kinetic parameter K_{Ox} was adjusted by a least-square method. The results reported in Table

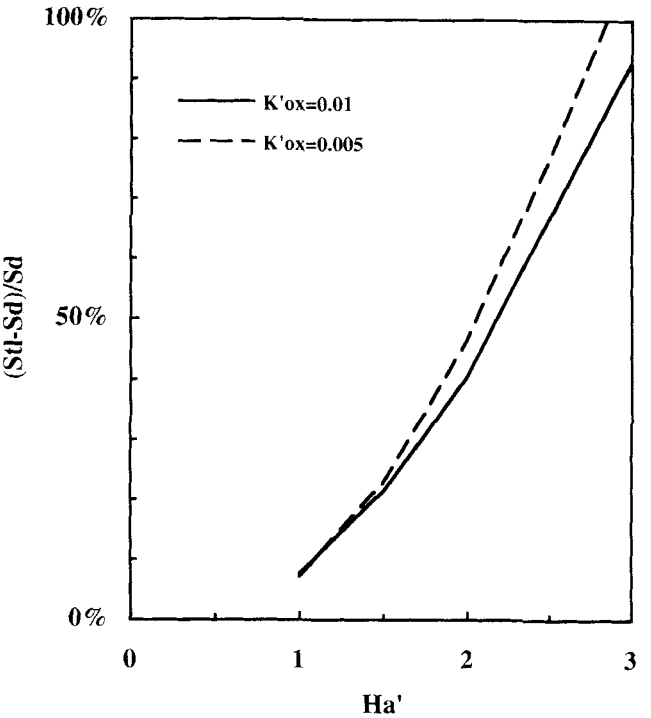

Figure 8. Relative error on the slopes of the $\bar{S}/T$ curves between the thin-layer and diffusive models.

Theoretical ratio $((S_{tl} - S_d)/S_d)/Ha'$ curves for different values of K'_{Ox} where S_{tl} is the slope determined with the thin-layer model and S_d with the diffusive one. $D = 0.2$, $\gamma = 0.5$, $\mathrm{Red}^0 = 0.01$, and $K'_S = 0.014$.

Table 4. Kinetic Parameter K_{Ox} Determined by the Least-Square Method Applied to the Thin-Layer Model

$k_e[E]$(mM·s^{-1})	K_{Ox} (mM)
0.017	0.36
0.069	0.95
0.174	1.67

$Red^0 = 0.01$.

4 give unreliable values of K_{Ox}. In particular it was not possible to fit all the curves with the same value of K_{Ox}. As indicated by the theoretical evaluation of the discrepancy between the two models (Figure 8), the thin-layer hypothesis is not valid, even if each curve, considered separately, could be consistent with a thin-layer behavior at first glance. The lines on Figure 7 represent the theoretical results obtained with the diffusive model. All the experimental curves were satisfactorily fitted with the same value of the only parameter to be adjusted, $K_{Ox} = 0.056$ mM.

Conclusion

Thin-layer electrochemical reactors are widely used as analytical tools. The present results emphasized the restricted domain of validity of the thin-layer hypothesis when the study of a homogeneous reaction is concerned. Whatever the method chosen to process the experimental data, and even using a sloppy criterion, it was not possible to significantly broaden the suitability of the thin-layer hypothesis for Hatta numbers greater than a few units. The best way for processing experimental data by means of the thin-layer model seems to only take into account the last part of the reaction and thus avoid the onset where the thin-layer hypothesis is only valid for the slowest homogeneous reactions. The rate of the heterogeneous electrochemical reaction could also affect the overall reaction rate, as demonstrated experimentally with the oxidation of hexacyanoferrate II, although this mediator is currently well-known as a fast electrochemical system. The case of the enzymatic reaction also demonstrated that the thin-layer hypothesis could be wrong even if the experimental data seemed to be well-fitted by the model for one experiment. It was found essential that a set of experimental results obtained under various operating conditions should be taken into account.

The thin-layer electrochemical reactors can be very efficient for a fast determination of the order of magnitude of homogeneous kinetics. A finer approach is nevertheless necessary as soon as the kinetics is no longer slow. The general model used here remained quite simple and led to a very good agreement with the experimental data. Even in this case, a thin-layer electrochemical reactor has a lot of advantages: there is a very low volume of solution required, a very high surface /volume ratio, electrical control, a coupling of optical and electrical information. Nevertheless the diffusivities of all the species involved must be determined prior to the kinetic study.

Notation

D_S, D_{Ox} = diffusivity of S and Ox, m^2·s^{-1}
E = potential of the electrode, V
$[E]$ = concentration of the enzyme, M
F = Faraday's constant, C·eq^{-1}
K'_S, K'_{Ox} = dimensionless Michaelis' constants, $K' = K/[S]^0$
n = number of electron exchanged, eq·mol^{-1}
$Ox = [Ox]/[S]^0$
r = homogeneous enzymatic rate, M·s^{-1}
$Red = [Red]/[S]^0$
S, Ox, Red = dimensionless concentrations $S = [S]/[S]^0$
T = dimensionless time, $T = t\ D_S/L^2$ (T designated the temperature only in Eqs. 20–22 and 36)
x = distance from the electrode, m
X = dimensionless distance from the electrode, $X = x/L$
γ = stoichiometric coefficient
ξ = dimensionless potential, $\xi = \exp\ [(nF/RT)\ (E - E'_0)]$, where T is the temperature

Superscript

0 = relative to the initial time

Literature Cited

Aizawa, M., R. W. Coughlin, and M. Charles, "Electrochemical Regeneration of Nicotinamide Adenine Dinucleotide," *Biochim. Biophys. Acta*, **385**, 362 (1975).

Astarita, G., *Mass Transfer with Chemical Reaction*, Elsevier, Amsterdam (1967).

Bard, A. L., and L. R. Faulkner, *Electrochemical, Methods, Fundamentals and Application*, Wiley, New York, p. 407 (1980).

Barman, T. E., *Enzyme Handbook*, Vol. 11, Springer-Verlag, Berlin-Heidelberg, p. 203 (1969).

Bauer, R., D. K. Friday, and D. J. Kirwan, "Mass Transfer and Kinetic Effects in an Electrode-Driven Homogeneous Reaction," *Ind. Eng. Chem. Fundam.*, **20**, 141 (1981).

Bond, A. M., and H. A. O., Hill, "Electrochemical Investigation of Metalloproteins and Enzymes Using a Model Incorporating Microscopic Aspects of the Electrode-Solution Interface," *Met. Ions Biol. Syst.*, **27**, 431 (1991).

Brett, A. M. C. F. O., "Design and Electrochemical Evaluation of an Optically Transparent Thin Layer Electrode Flow Cell," *Electroanalysis*, **4**, 911 (1992).

Charpentier, J. C., "Mass-Transfer Rates In Gas-Liquid Absorbers and Reactors," in *Advances in Chemical Engineering*, Vol. 11, T. B. Drew, ed., Academic Press, New York, p. 1 (1981).

Chen, J. K., and K. Nobe, "Oxidation of Dimethylaniline by Horseradish Peroxidase and Electrogenerated Peroxide," *J. Electrochem. Soc.*, **140**, 299 (1993).

Cornelisse, R., A. A. C. M., Beenackers, F. P. H. van Beckum, and W.P. M. van Swaaij, "Numerical Calculation of Simultaneous Mass Transfer of Two Gases Accompanied by Complex Reversible Reactions," *Chem. Eng. Sci.*, **35**, 1245 (1980).

Danckwerts, P. V., *Gas-Liquid Reactions*, McGraw-Hill, New York (1970).

Durliat, H., "Mise au Point d'une Électrode à Enzyme pour le Dosage du Lactate Sanguin," Thesis, Univ. of Toulouse, Toulouse, France (1975).

Golub, D., and Y. Oren, "Graphite Felt as an Electrode for Thin-Layer Electrochemistry," *J. Appl. Electrochem.*, **20**, 877 (1990).

Grossman, G., "Heat and Mass Transfer in Film Absorption," *Handbook of Heat and Mass Transfer*, Vol. 2, N. P. Cheremisinoff, ed., Gulf Publishing, Houston, p. 211 (1986).

Gui, J. Y., G. W. Hance, and T. Kuwana, "Long Optical Pathlength Thin Layer Spectroelectrochemistry: Study of Homogeneous Chemical Reactions," *J. Electroanal. Chem.*, **309**, 73 (1991).

Heineman, W. R., B. J. Norris, and J. F. Goelz, "Measurement of Enzyme $E^{0'}$ Values by Optically Transparent Thin Layer Electrochemical Cells," *Anal. Chem.* **47**, 79 (1975).

Hubbard, A. T., and F. C. Anson, "Thin Layer Electrochemical Cells," in *Electroanalytical Chemistry*, Vol. 4, A. J. Bard, ed., Marcel Dekker, New York, p. 129 (1970).

Kawiak, J., T. Jedrai, and T. Galus, "A Reconsideration of the Kinetic Data for $Fe(CN)_6^{3-}$/ $Fe(CN)_6^{4-}$ System," *J. Electroanal. Chem.*, **145**, 163 (1983).

Labrune, P., and A. Bergel, "Modelling of an Indirect Electrosynthesis Process: I. Theoretical Study of the Effect of Dismutation of the Mediator," *Chem. Eng. Sci.*, **47**, 1219 (1992).

Laviron, E., "General Expression of the Linear Potential Sweep Voltammogram in the Case of Diffusionless Electrochemical Systems," *J. Electroanal. Chem.*, **101**, 19 (1979).

Lortie, R., A. Fassouane, J.-M. Laval, and C. Bourdillon, "Displacement of Equilibrium in Electroenzymatic Reactor for Acetaldehyde Production Using Yeast Alcohol Dehydrogenase," *Biotechnol. Bioeng.*, **39**, 157 (1992).

Nagy, T. R., and J. L. Anderson, "Long Optical Path Thin-Layer Spectroelectrochemistry in a Liquid Chromatographic Ultraviolet-Visible Absorbance Detector Cell," *Anal. Chem.*, **63**, 2668 (1991).

Porter, M. D., and T. Kuwana, "Glassy Carbon and Graphite Electrodes with a Hole for Long Path Length Thin-Layer Spectroelectrochemistry," *Anal. Chem.*, **56**, 529 (1984).

Salbeck, J., "Spectroelectrochemical Thin Layer Cell for Nonaqueous Solvent Systems," *Anal. Chem.*, **65**, 2169 (1993).

Salbeck, J., "An Electrochemical Cell for Simultaneous Electrochemical and Spectroelectrochemical Measurements under Semi-infinite Diffusion Conditions and Thin Layer Conditions," *J. Electroanal. Chem.*, **340**, 169 (1992).

Trambouze, P., "Mass Transfer with a Chemical Reaction," in *Multiphase Chemical Reactors*, Vol. 1, A. E. Rodrigues, J. M. Calo, and N. H. Sweed, eds., Sijthoff and Noordhoff, Rockville, MD, p. 133 (1981).

Turner, A. P. F., I. Karube, and G. S. Wilson, *Biosensors Fundamentals and Applications*, Oxford Univ. Press, Oxford (1987).

Tzedakis, T., A. Savall, and M. J. Clifton, "The Electrochemical Regeneration of Fenton's Reagent in the Hydroxylation of Aromatic Substrates: Batch and Continuous Processes," *J. Appl. Electrochem.*, **19**, 911 (1989).

Weast, R. C., M. J. Astle, and W. H. Beyer, *Handbook of Chemistry and Physics*, 68th ed., CRC Press, Boca Raton, F-47 (1987).

Wei, W., Q. Xie, and S. Yao, "Theory and Application of Analytical Spectroelectrochemistry with Long Path Length Spectroelectrochemical Cells. Part I. Integral Equation Connecting the Absorbance with the Concentration Distribution and its Use in Digital Simulation for Long Path Length Thin Layer Spectroelectrochemical Cells," *J. Electroanal. Chem.*, **328**, 9 (1992); Erratum, *ibid.* **356**, 321 (1993).

Weise, L., G. Valentin, and A. Stork, "Selectivity Analysis in Electrochemical Reactors. II. Engineering Models of a Batch Reactor with a Complex Reaction Sequence," *J. Appl. Electrochem.*, **16**, 851 (1986).

Yao, C. L., F. J. Capdevielle, K. M. Kadish, and J. L. Bear, "Thin Layer Microcell for Transmittance Fourier Transform Infrared Spectroelectrochemistry," *Anal. Chem.*, **61**, 2805 (1989).

Yih, S. M., "Modeling Heat and Mass Transport in Falling Liquid Films," in *Handbook of Heat and Mass Transfer*, Vol. 2, N. P. Cheremisinoff, ed., Gulf Publishing, Houston, p. 111 (1986).

Manuscript received May 17, 1994, and revision received Oct. 13, 1994.